# PREDICTION OF THE EFFECTIVE DIFFUSIVITY OF WATER INSIDE CNT-BASED PMMA MEMBRANES

**Mermigkis G. Panagiotis[1], Dimitrios G. Tsalikis[1] and Vlasis G. Mavrantzas[1,2]**

[1]Department of Chemical Engineering
University of Patras
Patras, GR-26504, Greece
e-mail: mermigkis@chemeng.upatras.gr

[2]Department of Mechanical and Process Engineering
ETH-Z
Zürich, CH-8092, Switzerland
e-mail: vlasis@chemeng.upatras.gr

**Keywords:** Membranes, diffusion, carbon nanotubes, kinetic Monte Carlo.

**Abstract.** *We present computational results obtained from kinetic Monte Carlo (kMC) simulations for the effective diffusivity of water $D_{eff}$ inside PMMA membranes containing Carbon Nanotubes (CNTs) and their dependence on CNT volume concentration C in the matrix, CNT length L, and CNT diameter D. The simulation results are further mapped onto an algebraic equation which is found to describe very accurately the dependence of $D_{eff}$ on CNT aspect ratio L/D, volume concentration C, and orientation (random versus aligned) in the PMMA matrix.*

## 1 INTRODUCTION

As has been shown by numerous experimental and simulation studies, CNTs hold promise for the design of low fouling polymeric membranes due to their potential for attaining both high water flux and high rejection of low molecular weight organic pollutants [1-4]. This is of great interest in several technological processes and applications such as water desalination [5], membrane transportation [6], and separation and purification [7,8]. From a theoretical or simulation's point of view, most of the work so far has been concerned with water diffusivity or transport through CNTs as a function of CNT diameter [9,10]. From a practical point of view, however, equally (if not more) important is the ability to estimate the effective diffusivity of small molecules (like water) through the entire CNT-based polymer membrane. This requires a multi-scale simulation strategy, since diffusive rates through nanostructured membranes at room temperature correspond to time scales that considerably exceed those that can be accessed today by a brute force application of the molecular dynamics (MD) method. The situation is more complicated if we further consider the heterogeneity of a CNT-polymeric membrane, especially for long and/or large CNTs.

In this work, we present an efficient methodology for computing the effective diffusivity of water through CNT-PMMA membranes by following a hierarchical approach entailing three steps: a) First, atomistic MD simulations are executed in order to obtain the water diffusivity inside a CNT at room conditions as a function of its diameter; b) Second, atomistic MD simulations of water inside the pure polymer matrix (here PMMA) are performed to compute the water diffusion coefficient in PMMA as a function of temperature. Due to long times accompanying diffusion of small molecules in polymer matrices at low temperatures, the simulations here are executed at relatively high temperatures, and then the results are extrapolated down to room temperature ($T$=300K); c) Third, the results of steps (a) and (b) are utilized in the framework of a stochastic kMC algorithm to obtain the effective diffusivity $D_{\text{eff}}$ of water inside the entire CNT-PMMA matrix as a function of CNT diameter and aspect ratio, and CNT concentration (% volume fraction) in the membrane. This work focuses mainly on step (c).

## 2 SIMULATION METHOD

Kinetic Monte Carlo (kMC) method is a computer simulation Monte Carlo method intended to simulate the time evolution of several processes occurring in nature given the knowledge of their rates. These rates are inputs to the kMC algorithm, since the method itself cannot predict them; kMC is therefore similar to the dynamic Monte Carlo method presented by Gillespie [11,12]. In our work, the kMC algorithm is realized on a discrete 3d

cubic lattice with dimensions large enough so as to ensure that "finite system size effects" are absent. It is characterized by the following features:

- Lattice sites representing the nanocomposite membrane (PMMA+CNT) belong to three domains: the PMMA matrix, the interior of the CNTs, and the CNT faces (the entrance and exit regions). Lattice sites belonging to the CNT faces are the only ones through which a water molecule (a walker) can move from a PMMA site to a site inside a CNT and vice versa. That is, in our simulations, water molecules are allowed to enter or exit a CNT only through its two faces; lateral penetrations are strictly forbidden.
- The lattice spacing $d$ (distance between neighboring sites) is constant and the same in all domains, equal to the average jump length for the walker. Unless otherwise stated, the value of $d$ in all of our simulations was taken equal to 1 Å.
- Under equilibrium conditions, all lattice sites are assigned the same potential energy implying a uniform (homogeneous) distribution for the occupancy probability of a site. This is in contrast, e.g., to an earlier study of kinetic and spatial heterogeneities in the diffusion of small molecules in disordered media [13], where a Gaussian distribution of potential energies was assumed (implying a log-normal distribution for the occupancy probability).
- To each site, a rate constant $k_{ij}$ is assigned for a water molecule that is found in site $i$ to hop (diffuse) to a neighboring site $j$. For a cubic lattice, the number of neighboring sites is six (6) and are all equivalent.
- To the sites of the 3d-lattice, a large number of walkers is randomly distributed, and these can hop from one site $i$ to another $j$ with a rate whose value $k_{ij}$ is different for sites belonging to PMMA and CNT regions. These values are determined by the corresponding diffusivity values of water molecules in a pure PMMA matrix and in a CNT through the following relations:

$$r_{\text{PMMA-PMMA}} = \frac{D_{\text{PMMA}}}{d^2} \tag{1}$$

$$r_{\text{CNT-CNT}} = \frac{D_{\text{CNT}}}{d^2} \tag{2}$$

  where $r_{\text{PMMA}}$ denotes the transition rate from a PMMA site to another PMMA site and $r_{\text{CNT}}$ the corresponding transition rate from a CNT site to another CNT site. We recall that all transitions from a CNT site to a PMMA site or from a PMMA to a CNT one are forbidden except those taking place through the CNT faces (the entrance and exit areas). We further note that in our simulations lattice sites belonging to the two faces of each CNT are assigned a rate constant equal to $r_{\text{CNT}}$ for transitions to neighboring (facial or interior) CNT sites and a rate constant equal to $r_{\text{PMMA}}$ for transitions to neighboring PMMA sites.
- Periodic boundary conditions apply along all three space directions.

In our work, all CNTs were considered to be rectilinear, i.e., to have the shape of thin cylinders whose size is quantified by the diameter $D$ and axial length $L$. Our results below will thus be presented as a function of CNT size (CNT diameter $D$ and length $L$) and CNT concentration $C$. The latter was varied from $C$=2 % vol. to 30 % vol. We further distinguished between two CNT configurations in the polymer matrix: *random* and *aligned*. In the random configuration, CNTs are randomly placed inside the simulation cell both as far as the position of their center-of-mass and their axial direction are concerned. In the aligned configuration, CNTs are randomly placed inside the simulation cell only as far as their centers-of-mass are concerned but all of them point to the same direction (in our case, this was taken to be the direction of the $z$ axis of the coordinate system). Situations where one CNT crosses another CNT were excluded. As far as the two diffusivities ($D_{\text{PMMA}}$ and $D_{\text{CNT}}$) at $T$=300K are concerned, the following values were used in the calculations [14,15,16]: $D_{\text{CNT}} = 2.3\times10^3$ nm$^2$/μs and $D_{\text{PMMA}} =$ 1.3 nm$^2$/μs. From the above $D_{\text{CNT}}$ and $D_{\text{PMMA}}$ values, it is obvious that water molecules diffuse (travel) almost 1000 times faster inside CNTs than in the PMMA region of the membrane and our task in this project is to compute their overall or effective diffusivity $D_{\text{eff}}$ in the CNT-PMMA nanocomposite.

Our algorithm proceeds as follows: at each KMC step a complete list of possible jumps for all surface sites is constructed, and then a hopping event $j$ is randomly selected according to the following equation:

$$\frac{\sum_{i=1}^{i=j-1} r_i}{R} < \xi_1 < \frac{\sum_{i=1}^{i=j} r_i}{R} \tag{3}$$

where

$$R = \sum_{i=1}^{i=M} r_i \tag{4}$$

denotes the sum of the rate constants over all sites occupied by water molecules. Here $\xi_1$ is a random number generated from a uniform distribution in the interval (0, 1], $M$ denotes the total number of possible reaction (=hopping) events at present step, and $r_i$ is the reaction rate of the $i^{th}$ event. The corresponding time increment $\delta t$ through this kMC step is calculated through

$$\delta t = -\frac{\ln(\xi_2)}{R} \tag{5}$$

where $\xi_2$ is another random number uniformly generated in the interval (0,1]. The new time at the end of the kMC step will thus be:

$$t_{\text{new}} = t_{\text{old}} + \delta t \tag{6}$$

In the next kMC step, the total list of possible events for a walker site is updated based on the new configuration and the same procedure is carried on. And all this is continued for as many times as needed until the system enters the regime of Fickian diffusion from which one can reliably calculate diffusivities. Thus, the process of advancing ghost walkers is repeated in the simulation for a large number of time steps, and eventually we compute the mean square displacement $<r^2>$ (as an average over all walkers and all possible time origins) as a function of time $t$. The desired effective diffusion coefficient is computed from the slope of the $<r^2>$-vs.-$t$ curve in the linear (Fickian) regime by using the Einstein equation:

$$D_{eff} = \lim_{t\to\infty}\{\frac{1}{6t} < [r(t) - r(0)]^2 >\} \tag{7}$$

For Eq. (7) to yield reliable results, long simulation runs are required to ensure that the diffusive motion of the walkers has entered the regime of Fickian diffusion. To reduce the statistical uncertainty of the computed effective water diffusivity, we used a large number of walkers (about 5,000) and rather large simulation cells (of size 1nm x 1nm x 1nm in some cases). As far as the size and concentration of CNT addressed in our simulations are concerned, we worked with three different diameters ($D$=1nm, 1.2nm, 2nm), several lengths corresponding to aspect ratios equal to $L/D$=2.5, 5.0, 10, 15, 25, and 42, and many concentrations $C$ (ranging from 2% vol. to 30% vol.). We also studied the effect of CNT orientation (random vs. aligned CNTs) inside the PMMA matrix.

As a validation test, we simulated the effective diffusivity of water inside a PMMA matrix containing no CNTs to verify that we recover the value $D_{\text{PMMA}}$ assumed in the calculations.

## 3 RESULTS

*A. CNTs of Random direction*

We conducted 29 simulations of various CNT-PMMA systems consisting of a large number of randomly dispersed CNTs, and we studied the dependence of $D_{\text{eff}}$ on CNT aspect ratio $L/D$ (= CNT length / CNT diameter) and CNT volume percent concentration $C$ in the nanocomposite. In Table 1, we present the lengths of the cells and the number of CNTs in the matrix, for each pair of $C$ and $L/D$ simulated, while a typical geometric configuration of the simulated lattice structures for completely randomly distributed CNTs is shown in Fig. 1.

*Table 1*. Technical details (number of CNTs and cell lengths) of the simulated systems for the case of randomly distributed CNTs.

| | *L/D=2.5* | *L/D* = 5 | *L/D* = 10 | *L/D* = 15 | *L/D* = 25 | *L/D* = 42 |
|---|---|---|---|---|---|---|
| | CNTs=4 | CNTs = 11 | CNTs = 44 | CNTs = 101 | CNTs = 251 | CNTs = 697 |
| Concentration (%) | Lx(nm) | Lx (nm) | Lx (nm) | Lx (nm) | Lx (nm) | Lx (nm) |
| 2 | 13.0 | 13.4 | 29.4 | 40.7 | 81.4 | – |
| 5 | 9.6 | 9.9 | 20 | 30 | 60 | 100 |
| 10 | 7.6 | 7.8 | 15.8 | 23.8 | 47.6 | 79.4 |
| 15 | 6.7 | 6.8 | 13.9 | 20.8 | 41.6 | – |
| 20 | 6.0 | 6.2 | 12.6 | 18.9 | – | – |
| 25 | 5.6 | 5.8 | – | – | – | – |
| 30 | 5.3 | – | – | – | – | – |

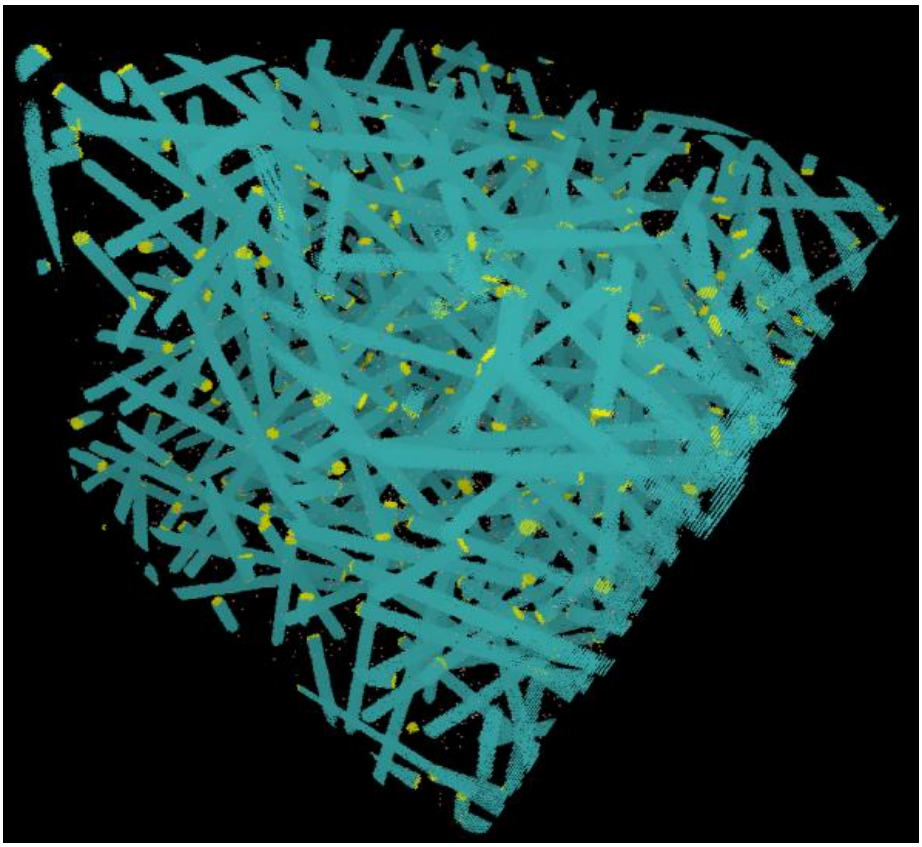

*Figure 1*: A typical snapshot of the initial configuration of a PMMA matrix filled with a large number (=697) of randomly placed CNTs.

All simulation results for the dependence of $D_{eff}$ on CNT aspect ratio $L/D$ and concentration $C$ are presented in Figures 2(a) and 2(b). They show that $D_{eff}$ increases as $L/D$ increases or as $C$ increases. The higher $D_{eff}$ values are observed in the simulations with the larger aspect ratio $L/D$; e.g., the values of $D_{eff}$ in the simulations with $C$=30% for $L/D$=2.5 and $L/D$=5 are significantly lower than those for $L/D$=42 in the CNT-PMMA membranes with $C$=5%.

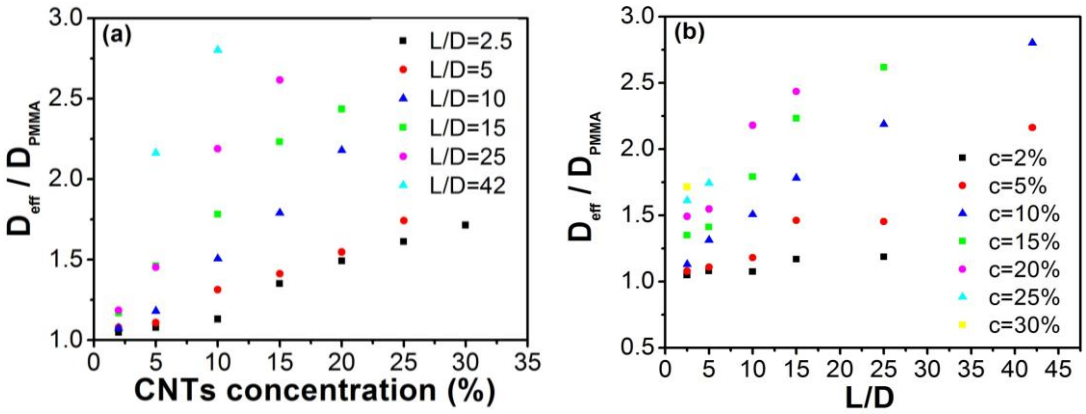


*Figure 2*: Dependence of $D_{eff}$ / $D_{PMMA}$ on (a): CNT concentration (for given $L/D$), and (b): CNT aspect ratio $L/D$ (for given $C$).

In the range of conditions analyzed in this work, and for a given concentration $C$ in CNTs, the kMC simulation demonstrate that $D_{eff}$ depends linearly on $L/D$. This result is of great importance since it suggests that, for a given concentration $C$ of the polymer-CNT membrane in CNTs, one can obtain larger water permeabilities by using thin and long CNTs, although from a technological point of view matrices with a high concentration in CNTs might be difficult or expensive to construct. We should also note that higher matrices with high CNT concentrations might be more prone to mechanical failure, especially in the presence of flow.

*B. Aligned CNTs*

To study the role of CNT configuration inside the membrane on $D_{\text{eff}}$ we carried out additional kMC simulations at several concentrations and for many different aspect ratios, but with all CNTs now in the simulation cell placed along the z direction. Such a configuration is useful since it can provide information for the effect that vertically aligned CNTs affect the mobility of water molecules inside the membrane. In Table 2, we provide some technical information about the simulated systems, such as the size of the cells, the number of CNTs in the matrix, and the values of $C$ and $L/D$. A typical geometric configuration of the simulated lattice structures for fully aligned CNTs is shown in Fig. 3.

*Table 2*. Technical details (number of CNTs, cell size, CNT length $L$, and CNT diameter $D$) of the simulated systems for the case of fully aligned CNTs in the PMMA matrix.

| | $L/D$ = 2.5 | $L/D$ = 5 | $L/D$ = 10 | $L/D$ = 15 | $L/D$ = 25 | $L/D$ = 42 |
|---|---|---|---|---|---|---|
| | No of CNTs = 3 | No of CNTs = 8 | No of CNTs = 49 | No of CNTs = 111 | No of CNTs = 312 | No of CNTs = 861 |
| Concentration (%) | $L_x = L_y = L_z$ (nm) | $L_x = L_y = L_z$ (nm) | $L_x = L_y = L_z$ (nm) | $L_x = L_y = L_z$ (nm) | $L_x = L_y = L_z$ (nm) | $L_x = L_y = L_z$ (nm) |
| 2 | 15 | 13.4 | 27.1 | 40.7 | 81.4 | — |
| 5 | 11.1 | 9.9 | 20 | 30 | 60 | 100 |
| 10 | 7.8 | 7.8 | 15.8 | 23.8 | 47.6 | 79.4 |
| 15 | 6.8 | 6.8 | 13.8 | 20.8 | 41.6 | 69.2 |
| 20 | 6.2 | 6.2 | 12.6 | 18.9 | 37.8 | 63 |
| 25 | 5.8 | 5.8 | 11.5 | 17.5 | 35 | 58.4 |
| 30 | 5.4 | 5.4 | 11 | 16.5 | 33 | 55 |

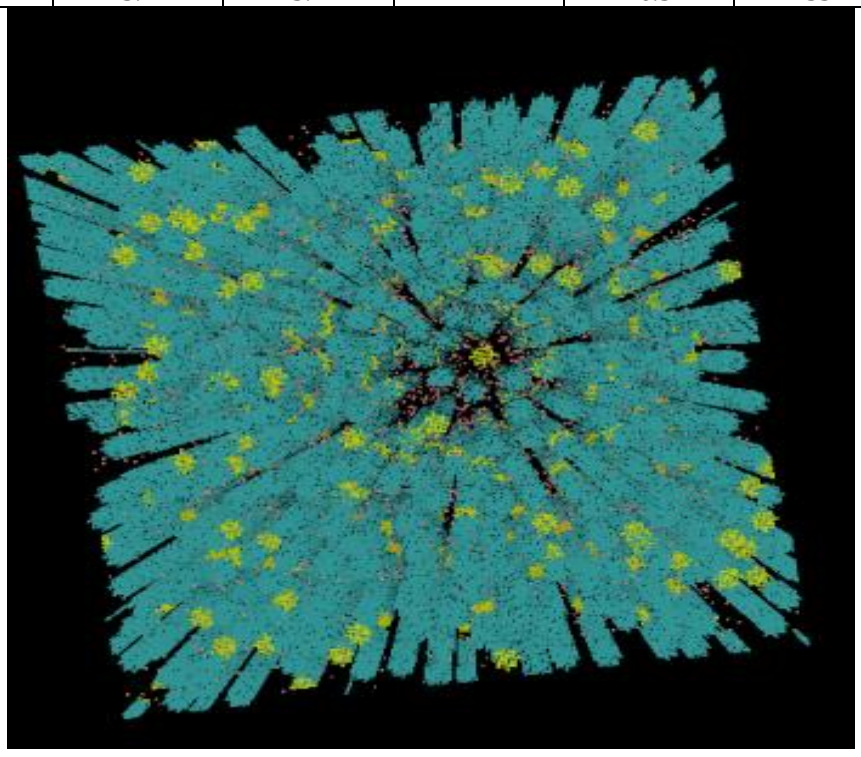

*Figure 3*: Typical snapshot of the initial configuration of a simulation cell containing a large number (=861) of fully aligned CNTs in the PMMA matrix.

Collectively, our simulation predictions for the dependence of $D_{\text{eff}}$ on CNT aspect ratio $L/D$ and concentration $C$ for the case of fully aligned CNTs are presented in Figures 4(a) and 4(b). The major conclusión is that CNT orientation does not have a significant effect on the effective water diffusivity in the membrane, in the sense that this still attains values that are higher (than those obtained with the random configuration) but always of the same

order of magnitude as the water diffusivity in pure PMMA. Similar to the case of random CNTs, the largest $D_{\text{eff}}$ values recorded in the kMC simulations correspond to systems characterized by the largest aspect ratio (e.g., $L/D$=42 at $C$=30%vol.), and it is 7 times larger than the diffusivity of water in a pure PMMA.

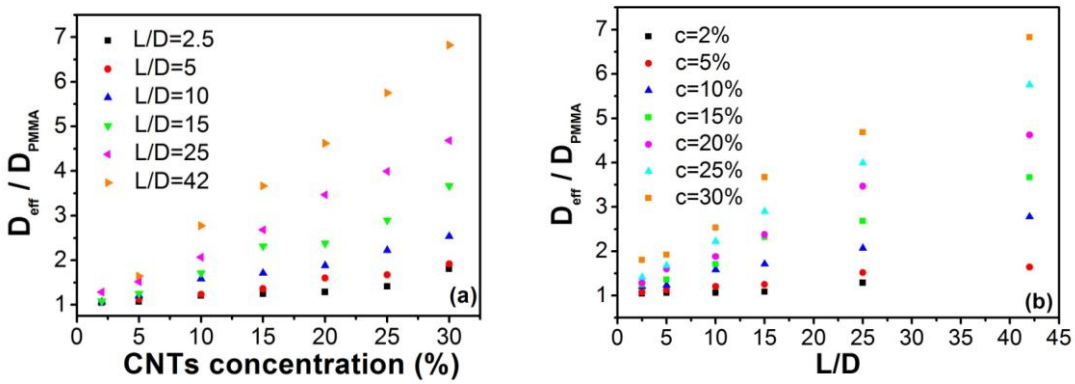


*Figure 4*: Dependence of $D_{\text{eff}}$ / $D_{\text{PMMA}}$ on (a): CNT concentration (for a given $L/D$ value) and (b): CNT aspect ratio $L/D$ (for a given CNT concentration $C$), for fully aligned CNTs.

*C. Analytical model*

From Figures 4(a) and 4(b) we also conclude that $D_{\text{eff}}$ tends to vary linearly both with CNT concentration and aspect ratio $L/D$. Based on this observation, we can propose a simple mathematical formula that can be used to get estimates of $D_{\text{eff}}$ for other conditions of $L/D$ and $C$ than those addressed here. By computing the slopes and intercepts of the corresponding linear fits in Figures 4(a),(b), we came up with the following algebraic equation describing the dependence $D_{\text{eff}}$ on $L/D$ and $C$ [17]:

$$\frac{D_{\text{eff}}(\frac{L}{D},\text{C})}{D_{\text{PMMA}}} = 0.0043C\frac{L}{D} + 0.00971C - 0.00241\frac{L}{D} + 0.983846 \quad (8)$$

It turns out that this closed-form expression describes quite accurately all simulation data for $L/D > 2.5$ and concentration $C > 2\%$, the largest deviation being less than 4%. In addition, it can be used to get a prediction for $D_{\text{eff}}$ in any CNT-based PMMA matrix y just knowing or providing the values of the aspect ratio $L/D$ and volume fraction $C$ of CNTs in the matrix.

## 4 CONCLUSIONS

We have used kMC simulations to study the effective diffusivity of water molecules inside a nanocomposite membrane consisting of a polymer matrix (PMMA) and CNTs, as well as its dependence on CNT aspect ratio, CNT concentration, and CNT orientation in the matrix. We conducted more than 70 simulations for randomly placed and aligned CNTs covering a large window of aspect ratios and concentrations. Our simulation results indicate that under equilibrium conditions (zero applied pressure gradient), the CNT orientation does not affect the effective diffusivity of water inside the membrane. We further found that the effective diffusivity depends linearly both on CNT concentration $C$ (keeping $L/D$ constant) and CNT aspect ratio $L/D$ (keeping $C$ constant). On the basis of these observations, we further reported a simple analytical expression for $D_{\text{eff}}$ as a function of $L/D$ and $C$.

## REFERENCES

[1] M. Majumder, N. Chopra, R. Andrews, B.J. Hinds, *Nature* 438, 44 (2005).
[2] M. Majumder, N. Chopra, B.J. Hinds, *ACS Nano* 5, 3867 (2011).
[3] J.K. Holt, H.G. Park, Y. Wang, M. Stadermann, A.B. Artyukhin, C.P. Grigoropoulos, A. Noy, O. Bakajin, *Science* 312, 1034 (2006).
[4] A. Kalra, S. Garde, G. Hummer, *Proc. Natl. Acad. Sci. (USA)* 100, 10175 (2003).
[5] B. Corry, *J. Phys. Chem. B* 112, 1427 (2008).

[6] K. Zhao, H. Wu, *J. Chem. Phys. B* 116, 13459 (2012).
[7] B.J. Hinds, N. Chopra, T. Rantell, R. Andrews, V. Gavalas, L.G. Bachas, *Science* 303, 62 (2004).
[8] J. Lee, N.R. Aluru, *Appl. Phys. Lett.* 96, 133108 (2010).
[9] K. Koga, G.T. Gao, H. Tanaka, X.C. Zeng, *Nature* 412, 802 (2001).
[10] A. Striolo, A.A. Chialvo, K.E. Gubbins, P.T. Cummings, *J. Chem. Phys.* 122, 234712 (2005).
[11] D.T. Gillespie, *J. Comp. Phys.* 22, 403 (1976).
[12] D.T. Gillespie, *J. Phys. Chem.* 81, 2340 (1977).
[13] N.Ch. Karayiannis, V.G. Mavrantzas, D.N. Theodorou, *Chem. Engin. Sci.* 56, 2789 (2001).
[14] A.B. Farimani, N.R. Aluru, *J. Phys. Chem. B* 115, 12145 (2011).
[15] A. Anastassiou, E. Karahaliou, O. Alexiadis, V.G. Mavrantzas, *J. Chem. Phys.* 139, 164711 (2013).
[16] M. Unemori, Y. Matsuya, S. Matsuya, A. Akashi, A. Akamine, *Biomaterials* 24, 1381 (2003).
[17] P.G. Mermigkis, D.G. Tsalikis, V.G. Mavrantzas, manuscript in preparation (2015).